



## **Sponge-derived fatty acids inhibit biofilm formation of MRSA and MSSA by down-regulating biofilm-related genes specific to each pathogen**

Title	Sponge-derived fatty acids inhibit biofilm formation of MRSA and MSSA by down-regulating biofilm-related genes specific to each pathogen
Author(s)	Khan, Neyaz A.;Barthes, Nicolas;McCormack, Grace;O'Gara, James P.;Thomas, Olivier P.;Boyd, Aoife
Publication Date	2023-07-19
Publisher	Oxford University Press and Applied Microbiology International
Repository DOI	<a href="https://doi.org/10.1093/jambio/lxad152">https://doi.org/10.1093/jambio/lxad152</a>

# Sponge-derived fatty acids inhibit biofilm formation of MRSA and MSSA by down-regulating biofilm-related genes specific to each pathogen

Neyaz A. Khan<sup>1</sup>, Nicolas Barthes<sup>2</sup>, Grace McCormack<sup>1</sup>, James P. O’Gara<sup>3</sup>, Olivier P. Thomas<sup>3</sup>, Aoife Boyd<sup>1,\*</sup>

<sup>1</sup>School of Natural Sciences and Ryan Institute, University of Galway, University Road Galway H91 TK33, Ireland

<sup>2</sup>Centre d’Ecologie Fonctionnelle et Evolutive, UMR 5175, CNRS, Université de Montpellier, Université Paul Valéry Montpellier, EPHE, IRD, F-34293 Montpellier, France

<sup>3</sup>School of Biological and Chemical Sciences, Ryan Institute, University of Galway, University Road Galway H91 TK33, Ireland

\*Corresponding author. School of Natural Sciences, University of Galway, University Road, Galway, H91 TK33, Ireland. E-mail: [Aoife.Boyd@UniversityOfGalway.ie](mailto:Aoife.Boyd@UniversityOfGalway.ie)

## Abstract

**Aim:** A promising approach for the development of next-generation antimicrobials is to shift their target from causing bacterial death to inhibiting virulence. Marine sponges are an excellent potential source of bioactive anti-virulence molecules (AVM). We screened fractions prepared from 26 samples of Irish coastal sponges for anti-biofilm activity against clinically relevant pathogens.

**Methods and results:** Fifteen fractions from eight sponge species inhibited biofilm of methicillin-susceptible *Staphylococcus aureus* (MSSA), methicillin-resistant *S. aureus* (MRSA), and/or *Listeria monocytogenes* without causing growth inhibition. Gas chromatograph/mass spectroscopy analyses of *Mycale contarenii* fractions revealed the presence of myristic acid and oleic acid. These fatty acids repressed transcription of the fibronectin-binding protein *fnbA* and *fnbB* genes and the polysaccharide intercellular adhesin *icaADBC* operon, which are required for MRSA and MSSA biofilm formation, respectively.

**Conclusions:** This study illustrates the potential of AVM from Irish coastal sponges to specifically target bacterial virulence phenotypes, in this case, repression of biofilm formation via decreased transcription of biofilm-associated genes in MSSA and MRSA.

## Significance and impact of the study:

Anti-biofilm activity is a prevalent characteristic of marine sponges, and sponge anti-virulence molecule, such as oleic and myristic acids, could be exploited to inhibit biofilm formation of clinical pathogens in medical or industrial settings.

**Keywords:** anti-virulence molecule, biofilm, *Staphylococcus aureus*, marine sponge, *Mycale contarenii*, myristic and oleic acid

## Introduction

Antimicrobial-resistant (AMR) pathogenic bacteria have become one of the major threats globally, and many conventional antibiotics have become ineffective against infectious microbes (Blair 2018). A promising approach for the development of next-generation antimicrobials is to shift their target from causing bacterial death to inhibiting virulence. Hence, this channels our attention to anti-virulence molecules (AVM), which impede virulence traits such as attachment to host tissue, biofilm formation, toxin activity and secretion, or bacterial communication systems. AVM are not bactericidal in action and so they do not exert selective pressure on bacteria for the development of AMR mutants (Werner et al. 2008).

Among the virulence factors, biofilm formation is a crucial trait possessed by bacteria that helps them to colonize their host and protects them from antibiotics, stress, and host immune response mediators and effectors. In the food industry, biofilms formed inside food processing facilities cause food spoilage, thereby affecting productivity and consumer health (Galie et al. 2018). In health-care settings,

biofilm formation on implantable devices such as joint implants, urinary catheters, heart catheters, and heart valves leads to persistent infections that are difficult to eliminate (Percival et al. 2015). Some of the most common biofilms formed in medical devices are those of Staphylococcal species (Chen et al. 2013).

The *Staphylococcus aureus* biofilm matrix comprises proteins, nucleic acids, and polysaccharides. Some of the most well-studied protein components are the ‘microbial surface components recognizing adhesive matrix molecules’ (MSCRAMMs), which facilitate bacterial attachment to host-derived extracellular matrix proteins. This group of adhesins includes fibronectin-binding proteins (FnBP), which attach to multiple host ligands, including fibronectin, and enhance host cell attachment and invasion (Taschner et al. 2002, O’Neill et al. 2008). In addition, FnBPA and FnBPB expressed by clinical methicillin-resistant *S. aureus* (MRSA) strains promote interactions between bacterial cells and biofilm development (O’Neill et al. 2008, Vergara-Irigaray et al. 2009). The genetic determinants and mechanisms of biofilm formation in MRSA and methicillin-susceptible *S. aureus* (MSSA) are independent

Received: January 6, 2023. Revised: June 9, 2023. Accepted: July 18, 2023

© The Author(s) 2023. Published by Oxford University Press on behalf of Applied Microbiology International. This is an Open Access article distributed under the terms of the Creative Commons Attribution-NonCommercial License (<https://creativecommons.org/licenses/by-nc/4.0/>), which permits non-commercial re-use, distribution, and reproduction in any medium, provided the original work is properly cited. For commercial re-use, please contact [journals.permissions@oup.com](mailto:journals.permissions@oup.com)

of each other: the *fnbA* and *fnbB* genes are primarily associated with MRSA protein-based biofilms, and the *icaA* and *icaR* genes with polysaccharide-based MSSA biofilms (McCarthy et al. 2015). Polysaccharide intracellular adhesin (PIA) is synthesized by products of the *icaABCD* operon, whose expression is negatively regulated by IcaR, a transcriptional repressor (Cafiso et al. 2004, Cue et al. 2009). In addition, a key regulator of *S. aureus* virulence, the accessory gene regulator (*agr*), which is a component of a quorum sensing system, negatively regulates biofilm production (Boles and Horswill 2008). Repression of the *agr* system is required for biofilm formation, as activation of this system increases extracellular protease production and promotes cell detachment from biofilms. The *agr* locus is itself regulated by *sarA* (staphylococcal accessory regulator A), a global regulator that controls the expression of various virulence factors, including positive regulation of biofilm formation in both MRSA and MSSA (Chien et al. 1999).

In our search for biofilm-targeting AVM, we focused on bioactive natural products produced by marine invertebrates collected off the Irish coasts, as they were available in our national marine biomaterial repository hosted at the University of Galway. Marine sponges produce a plethora of diverse bioactive molecules, including antibacterial compounds that play ecological roles in antimicrobial defences (Laport et al. 2009). However, very few molecules have shown direct and specific anti-biofilm activity that is not a result of bacteriostatic or bactericidal properties. To date, only three classes of natural products from marine sponges have been shown to specifically inhibit biofilm formation: terpenoids, pyroleimidazoles, and phorbaketals (Huigens et al. 2007, Rogers et al. 2010, Kim et al. 2021a).

In this study, we investigated the anti-biofilm activity of sponges collected from Irish coastal waters against MRSA, MSSA, *Pseudomonas aeruginosa*, *Listeria monocytogenes*, and *Vibrio parahaemolyticus*, which are pathogenic bacteria associated with severe diseases in humans and high rates of mortality and morbidity (Scallan et al. 2011, Serra et al. 2015). We further assessed AVM with anti-biofilm activity against both MRSA and MSSA and their ability to modulate transcription of biofilm matrix component genes.

## Materials and methods

### Reagents, bioactive molecules, bacterial strains, and growth conditions

All chemicals and reagents were sourced from Sigma-Aldrich, unless otherwise stated. Strains used in this study include MSSA 8325-4 (Novick 1967), MRSA BH1CC (O'Neill et al. 2007), BH1CC *fnbAB* (O'Neill et al. 2008), *L. monocytogenes* EGD-e (Glaser et al. 2001), *P. aeruginosa* PA01 (Holloway 1955), and *V. parahaemolyticus* RIMD2210633 (Makino et al. 2003). Apart from BH1CC *fnbAB*, these are biofilm-producing strains. All bacterial strains were cultivated in brain heart infusion (BHI) (Oxoid) media, with the addition of 3% NaCl for halophilic *V. parahaemolyticus*, and grown at 37°C.

### Collection of marine sponges and fraction preparation

Twenty-six sponge samples were collected, by hand for intertidal samples and by SCUBA for subtidal samples, from different regions of Irish coastal water in the context of the Irish

Marine Biomaterial Repository (Tables S1 and S2). Sponge species were taxonomically identified through morphological and spicule analysis (Picton and Morrow). Voucher specimens of each sample are maintained at the Irish Marine Biomaterial Repository ([www.imbd.ie](http://www.imbd.ie)) with identification through their BDV number (University of Galway, Marine Biodiscovery, Galway, Ireland).

After collection, sponge biomaterial was brought to the laboratory at  $-20^{\circ}\text{C}$  and freeze-dried. One g sponge biomaterial was extracted three times using a solvent mixture of 1:1 methanol (MeOH): dichloromethane ( $\text{CH}_2\text{Cl}_2$ ) and fractionated using solid phase extraction on  $\text{C}_{18}$ -bonded silica (Agilent 1 g BondElut  $\text{C}_{18}$  cartridges), eluting with varying solvent mixtures (1:1  $\text{H}_2\text{O}$ :MeOH, MeOH, and 1:1 MeOH: $\text{CH}_2\text{Cl}_2$ ) to produce three fractions: 1:1  $\text{H}_2\text{O}$ :MeOH ( $F_{\text{wm}}$ ), MeOH ( $F_{\text{m}}$ ), and 1:1 MeOH: $\text{CH}_2\text{Cl}_2$  ( $F_{\text{md}}$ ). The fractions were dried using a rotary evaporator (VirTis SP Scientific) and stored at  $-20^{\circ}\text{C}$ . Fractions were dissolved in dimethyl sulphoxide (DMSO) at a concentration of  $10\text{ mg ml}^{-1}$  and diluted to  $100\text{ }\mu\text{g ml}^{-1}$  for biological assays.

### Extraction and identification of the metabolites from the sponge *M. contarenii*

Freeze-dried *Mycale contarenii* (7.0 g) was extracted three times with 1:1 MeOH: $\text{CH}_2\text{Cl}_2$  to obtain extract (180 mg) after evaporation and fractionated by  $\text{C}_{18}$ -Vacuum Liquid Chromatography. The column was eluted in a step-wise manner to produce fractions of decreasing polarity:  $\text{H}_2\text{O}$  (F1), 1:1  $\text{H}_2\text{O}$ :MeOH (F2, 64 mg), 1:3  $\text{H}_2\text{O}$ :MeOH (F3, 7.6 mg), MeOH (F4, 2 mg), and 1:1 MeOH: $\text{CH}_2\text{Cl}_2$  (F5, 33 mg). The bioactive fractions were separated on a Waters X-Select CSH Phenyl-Hexyl column ( $5\text{ }\mu\text{m}$ ,  $4.6 \times 250\text{ mm}$ ) with a flow rate of  $1.0\text{ ml min}^{-1}$ . Initial elution was 1:2  $\text{H}_2\text{O}$ : $\text{CH}_3\text{CN}$  (+ 0.1% TFA) for 5 min and then followed by a linear gradient over 30 min to 100%  $\text{CH}_3\text{CN}$  (+ 0.1% TFA). The collected sub-fractions were identified using NMR and MS.

### Structure analysis using NMR

Nuclear Magnetic Resonance (NMR) experiments were performed on 500 MHz Varian Inova spectrometer with 5 mm OneNMR probe and 600 MHz Agilent Premium Compact spectrometer with 5 mm CryoProbe (Agilent, Santa Clara, USA). Chemical shifts ( $\delta$  in ppm) were referenced to the residual solvent peaks of the  $\text{CD}_3\text{OD}$  and  $\text{CDCl}_3$  carbon ( $\delta_{\text{C}}$  49.00 and 77.16, respectively) and proton ( $\delta_{\text{H}}$  3.31 and 7.26, respectively) signals. High-resolution mass spectra (HRESIMS) were obtained using Agilent 6540 QToF mass spectrometer equipped with Agilent 1290 UPLC and auto sampler (Agilent). Vacuum Liquid Chromatography fractionation was performed using polyoprep  $\text{C}_{18}$ -bonded silica 35–60  $\mu\text{m}$ , 120 Å (Labquip). Preparative High Performance Liquid Chromatography (HPLC) was carried out on Jasco HPLC system equipped with two PU-2087 pumps and UV-2075 detector. Analytical HPLC was carried out on Agilent 1260 HPLC system equipped with DAD and ELSD detector. All solvents used for extraction and separations were HPLC grade, and  $\text{H}_2\text{O}$  was milli-Q filtered.

### Gas chromatograph/mass spectroscopy analysis

Extracts were analysed using Shimadzu GCMS-QP2010plus (Shimadzu Scientific Instruments, Kyoto, Japan) equipped

with Optima-5MS column (30 m × 0.25 mm × 0.25 μm, Macherey-Nagel, Düren, Germany) at the Plateforme d'Analyses Chimiques en Ecologie, France. Helium was used as the carrier gas, at a constant 1 ml min<sup>-1</sup> flow rate. One microliter CH<sub>2</sub>Cl<sub>2</sub> solubilized extract was injected in a 270°C heated injection port. A split ratio of 1:4 was applied. The run had the temperature protocol: 100°C for 2 min, 100–200°C ramped at 10°C min<sup>-1</sup>, 200–270°C ramped at 10°C min<sup>-1</sup>, and finally held at 270°C for 1 min. The overall analysis lasted 20 min. The ion source and transfer line temperatures of the Mass Spectrometer were 225 and 270°C, respectively. Mass was scanned from *m/z* 38–400 in electron ionization mode. Chromatograms were analysed with MZmine2 (Pluskal et al. 2010). Identification of compounds was performed by comparison of mass spectra using the NIST library 2017 and cross-checking linear retention index. NIST-unknown analytes were annotated manually.

### Cytotoxicity assay

Cytotoxicity was quantified as previously described (Matlawska-Wasowska et al. 2010). HeLa cells were cultured in DMEM complete (Dulbecco's Minimal Eagles Medium-low glucose and without phenol red containing 10% (v/v) fetal bovine serum, 20 mmol l<sup>-1</sup> L-glutamine, 100 IU ml<sup>-1</sup> penicillin, 100 μg ml<sup>-1</sup> streptomycin) at 37°C, 5% CO<sub>2</sub>. For co-incubation experiments, cells were seeded at 20 000 cells ml<sup>-1</sup> DMEM complete per well in 48-well tissue culture plates. After 16 h, monolayers were washed with Phosphate-buffered saline (PBS-10 mM Na<sub>2</sub>HPO<sub>4</sub>/NaH<sub>2</sub>PO<sub>4</sub> Phosphate Buffer, 137 mM NaCl, 2.7 mM KCl, pH 7.4), and 500 μl DMEM was added per well with 100 μg ml<sup>-1</sup> sponge fractions. Non-treated cells acted as the 0% lysis control, and cells treated with 0.8% Triton X-100 were the 100% lysis control. After 6 and 24 h, cytotoxicity was determined through lactate dehydrogenase (LDH) assay using the Promega CytoTox 96 Non-Radioactive Cytotoxicity Assay kit, according to the manufacturer's directions, to measure lactate dehydrogenase released from lysed cells. Data are presented as means ± SD of three independent experiments.

### MIC broth dilution assay

Antimicrobial activity of the fractions was assessed by minimum inhibitory concentration (MIC) broth dilution assay according to the Clinical and Laboratory Standards Institute guidelines (CLSI 2015). Two hundred microliter overnight bacterial cultures adjusted to 0.001 OD<sub>595</sub> were inoculated in 96-well microtitre plates in Mueller-Hinton broth containing 2-fold serially diluted fractions (6–100 μg ml<sup>-1</sup>). Gentamicin was used as a positive control. Bacteria were incubated for 24 h at 37°C, and absorbance at 600 nm was measured using a microplate reader (Tecan, Austria) with Magellan software. Experiments were conducted thrice in triplicate.

### Biofilm assay

The ability of sponge fractions to inhibit biofilm formation of target pathogens was assessed by crystal violet staining, as described previously (Xu et al. 2016). Two hundred microliter overnight bacterial culture adjusted to 0.02 OD<sub>595</sub> was added to 96-well microtitre plates in the presence and absence of 100 μg ml<sup>-1</sup> sponge fractions for 24 h at 37°C. To en-

hance biofilm production by *S. aureus*, tissue culture-treated (delta surface) plates (Thermo Fisher) and growth media supplemented with 4% (w/v) NaCl (MSSA) or 1% (w/v) glucose (MRSA) were used (Vuong et al. 2000, Fitzpatrick et al. 2006). After 24 h, supernatant was discarded, and the biofilm was washed thrice with PBS. The biofilms were heat-fixed at 60°C for 1 h and stained with 0.1% crystal violet. The wells were washed thrice with PBS, and the stained biofilm was solubilized with 5% acetic acid. Absorbance was measured at OD<sub>595</sub>. The amount of biofilm is directly proportional to the optical density value (Xu et al. 2016). To determine if the sponge fraction reduced biofilm formation by inhibiting attachment, we monitored initial stages of biofilm formation by microscopy. For this purpose, after the biofilms were formed and then heat-fixed at 60°C as described above, the biofilms on the bottom of the wells of the microtitre plates were viewed on a Leica DFC 420 C inverted microscope with digital camera at 40X, and 10X magnification and brightfield images acquired.

### Growth curve

The effect of fatty acids on bacterial growth was determined by growing 200 μl overnight culture (adjusted to 0.02 OD<sub>600</sub>) in a 96-well plate at 37°C in BHI in the presence and absence of fatty acids (myristic acid, oleic acid, palmitic acid, and stearic acid) at concentrations of 25–100 μg ml<sup>-1</sup> for 14 h inside a microplate reader (LT-5000 MS ELISA reader). Cell growth was measured by optical density at 600 nm at 15-min intervals. These broth dilution experiments were performed thrice in triplicate.

### Gene expression analysis by quantitative PCR (qPCR)

For RNA isolation, MRSA and MSSA were cultured in growth conditions similar to those of the biofilm assay described above but in larger volumes. Four milliliter MRSA and MSSA at an initial turbidity of 0.02 at OD<sub>600</sub> were inoculated into BHI medium supplemented with 1% glucose (MRSA) and 4% NaCl (MSSA) in tissue culture-treated 12-well plates in the presence or absence of myristic acid or oleic acid at 25 μg ml<sup>-1</sup> and incubated at 37°C without shaking for the specified times. RNAProtect reagent (Qiagen) was added to the cells just before RNA cell harvest. Total RNA was isolated from 1.5 ml of 3 and 4 h culture (0.5 OD<sub>600</sub>) by bead beating with ZR BashingBead (Cambridge Biosciences) using FastPrep (MP Biomedical) for 60 s (×2) at 6 m s<sup>-1</sup>. The extracted RNA was purified using Qiagen RNeasy mini Kit (Qiagen) and DNase-treated with TURBO DNase (Invitrogen) for 30 min at 37°C. The DNase was inactivated by DNase inactivation reagent (5 min treatment). The solution was centrifuged for 1.5 min at 10 000 × g, and the supernatant containing RNA was collected. cDNA synthesis was carried out with random hexamer primer using First Strand cDNA Synthesis Kit (Roche). Real-time quantitative polymerase chain reaction (qPCR) was performed using SYBR Green master mix (Roche) with the cDNA to determine the transcript levels of *fnbA*, *fnbB*, *agrB*, and *sarA* genes in MRSA and *icaA*, *icaR*, *agrB*, and *sarA* genes in MSSA. The housekeeping gene *gyrB* was used to normalize the cycle threshold (Ct) values of all the tested genes, and Pfaffl method (Pfaffl 2001) was used to calculate differences in gene transcription. The qPCR data were expressed as fold changes in mRNA transcript levels of targeted genes in the

**Table 1.** Bioactive sponge fractions with cytotoxic or biofilm inhibition properties.

Sponge species	Fraction type <sup>a</sup>	% HeLa cell lysis		Anti-biofilm activity <sup>b</sup>	
		6 h	24 h	MSSA	<i>L. monocytogenes</i>
<i>Aplysilla rosea</i>	<i>F<sub>wm</sub></i>	6 ± 3	8 ± 3		+
<i>Clathria (Microcionia) strepsitoxa</i>	<i>F<sub>m</sub></i>	3 ± 2	5 ± 2	+++	
<i>Clathrina coriacea</i>	<i>F<sub>m</sub></i>	3 ± 2	16 ± 5		
<i>Cliona celata</i>	<i>F<sub>md</sub></i>	3 ± 2	12 ± 7		
<i>H. panicea</i>	<i>F<sub>wm</sub></i>	4 ± 2	5 ± 2	++	
<i>H. panicea</i>	<i>F<sub>m</sub></i>	2 ± 2	3 ± 1	++	
<i>H. panicea</i>	<i>F<sub>md</sub></i>	2 ± 1	4 ± 1	++	
<i>Haliclona fistulosa</i>	<i>F<sub>wm</sub></i>	3 ± 2	6 ± 2		++
<i>Halisarca dujardinii</i>	<i>F<sub>wm</sub></i>	3 ± 3	11 ± 5		
<i>H. dujardinii</i>	<i>F<sub>m</sub></i>	5 ± 3	30 ± 4		
<i>H. dujardinii</i>	<i>F<sub>md</sub></i>	7 ± 3	38 ± 9		
<i>Hemimycale columella</i>	<i>F<sub>wm</sub></i>	3 ± 1	23 ± 10		
<i>Hymeniacion perlevis</i>	<i>F<sub>md</sub></i>	7 ± 3	11 ± 2		
<i>Iophon hyndmani</i>	<i>F<sub>m</sub></i>	4 ± 2	13 ± 6		
<i>Mycale contarenii</i>	<i>F<sub>md</sub></i>	5 ± 1	7 ± 1	+++	
<i>M. rotalis</i>	<i>F<sub>wm</sub></i>	3 ± 2	6 ± 3	++	
<i>M. rotalis</i>	<i>F<sub>m</sub></i>	4 ± 1	4 ± 1		+
<i>M. rotalis</i>	<i>F<sub>md</sub></i>	4 ± 3	5 ± 2		++
<i>Pachymatisma johnstonia</i>	<i>F<sub>wm</sub></i>	2 ± 2	3 ± 0		+
<i>P. johnstonia</i>	<i>F<sub>md</sub></i>	6 ± 2	24 ± 5		+
<i>Polymastia penicillus</i>	<i>F<sub>m</sub></i>	8 ± 3	23 ± 6		
<i>Spongosorites calcicola</i>	<i>F<sub>wm</sub></i>	43 ± 8	61 ± 6	+++	+
<i>S. calcicola</i>	<i>F<sub>m</sub></i>	15 ± 6	17 ± 2	+++	+
<i>S. plumosum</i>	<i>F<sub>wm</sub></i>	1 ± 1	3 ± 1		++
<i>S. plumosum</i>	<i>F<sub>m</sub></i>	1 ± 1	5 ± 1	+++	
<i>Tethya citrina</i>	<i>F<sub>wm</sub></i>	3 ± 1	5 ± 4		+

Experiments were performed thrice in triplicate.

<sup>a</sup>*F<sub>wm</sub>* = fraction water: MeOH; *F<sub>m</sub>* = fraction MeOH; *F<sub>md</sub>* = fraction MeOH:CH<sub>2</sub>Cl<sub>2</sub>.

<sup>b</sup>+ = 20–49% reduction in biofilm formation; ++ = 50–90% reduction; +++ = >90% reduction; Empty cell = <20% reduction. Fractions which reduced both MSSA and MRSA biofilm production are in bold.

treated strains relative to their levels in the untreated bacteria. Primers (Table S3) were designed using Primer3 software (Rozen and Skaletsky 2000). The primer efficiency was determined using standard curve method (Ramakers et al. 2003). Transcription levels were determined using three independent cultures and two qRT-PCR reactions per gene.

### Statistical analysis

Data presented are the average values of three biologically independent experiments ± SD. *P*-values were calculated by Student's *t*-test comparing data for treated bacteria with data for control bacteria cultured with DMSO.

## Results

Specimens of 26 sponge species were collected from around the Irish coast (Table S1). Fifty-six fractions were prepared from the organic extracts of the sponge specimens using solid phase extraction on C18 and three successive solvent mixtures (MeOH, 1:1 H<sub>2</sub>O:MeOH, and 1:1 MeOH:CH<sub>2</sub>Cl<sub>2</sub>). Fractions that contained a sufficient quantity of material were assessed for bioactivity. These fractions were dried, re-suspended in DMSO, and tested for bioactivity at 100 µg ml<sup>-1</sup>.

### Cytotoxicity of sponge fractions toward HeLa cells

To identify AVM that are not cytotoxic, we assessed the ability of the fractions to kill cells of the HeLa human cancer line (Masters 2002). Table 1 displays the fractions with cytotoxic

or anti-biofilm activity. Fractions lacking both these characteristics are not included in this Table. After 6 h incubation with 100 µg ml<sup>-1</sup> sponge fractions, only *F<sub>wm</sub>* and *F<sub>m</sub>* of *Spongosorites calcicola* induced >10% lysis of HeLa cells (Table 1). *F<sub>wm</sub>* showed high toxicity toward HeLa cells with 43% cell lysis, whereas less toxicity was observed for *F<sub>m</sub>* with 15% cell lysis. After 24 h incubation, 12 sponge fractions caused >10% HeLa cell lysis with *F<sub>wm</sub>* of *S. calcicola* being the most cytotoxic by inducing 61% cell lysis, followed by *F<sub>m</sub>* and *F<sub>md</sub>* of *Halisarca dujardinii*, which caused 30 and 38% cell lysis, respectively.

### Anti-biofilm activity of sponge fractions

Prior to assessing the anti-biofilm activity of the sponge fractions, they were tested for their antibacterial activity against MSSA, *L. monocytogenes*, *V. parahaemolyticus*, and *P. aeruginosa* using the MIC broth dilution method. Only fractions of *S. calcicola* possessed antibacterial activity: *F<sub>wm</sub>* had an MIC of 6.25 µg ml<sup>-1</sup> for *S. aureus* and an MIC of 25 µg ml<sup>-1</sup> for *V. parahaemolyticus* and *L. monocytogenes*, while *F<sub>m</sub>* had an MIC of 100 µg ml<sup>-1</sup> for *S. aureus*. The antimicrobial activity of bis-indole alkaloid components of *S. calcicola* has since been biologically characterized (Jennings et al. 2019, Khan et al. 2022). As expected, bacteria treated with *S. calcicola* *F<sub>wm</sub>* or *F<sub>m</sub>* did not form biofilms due to the antimicrobial activity of these fractions (Table 1). Since the antimicrobial and anti-biofilm properties of the *S. calcicola* fractions could not be confidently differentiated, these fractions were not further analysed in this study. The absence of antibacterial activity in other fractions (MIC > 100 µg ml<sup>-1</sup>) indicated the

suitability of assessing their anti-biofilm activity against the target pathogens.

None of these fractions inhibited biofilm formation of *P. aeruginosa* or *V. parahaemolyticus*. Excluding *S. calicicola*, seven fractions displayed anti-biofilm activity against MSSA (Table 1). These seven fractions were then assessed for their ability to inhibit MRSA biofilm production, which showed that five fractions were active against both MRSA and MSSA (Fig. 1a and b)—*Clathria strepsitoxa* ( $F_m$ ), *M. contarenii* ( $F_{md}$ ),  $F_m$ , and  $F_{md}$  of *Halichondria panicea* and *Stylostichon plumosum* ( $F_m$ )—while *H. panicea* ( $F_{wm}$ ) and *M. rotalis* ( $F_{wm}$ ) inhibited biofilm formation of MSSA only (Fig. 1b). *Clathria strepsitoxa* ( $F_m$ ) and *M. contarenii* ( $F_{md}$ ) showed the strongest effect by inhibiting biofilm formation of both MRSA and MSSA by 90%. Eight fractions from six sponge species reduced biofilm formation by *L. monocytogenes* (Fig. 1c). Two of these sponge species (*M. rotalis* and *S. plumosum*) also possessed anti-biofilm activity against either MRSA or MSSA, but in a different fraction. *Mycale rotalis* ( $F_{md}$ ) and *S. plumosum* ( $F_{wm}$ ) showed the strongest *L. monocytogenes* biofilm inhibition at 63% and 60%, respectively (Fig. 1c).

This assessment showed that 15 fractions of nine sponge species had anti-biofilm activity. Five of the seven fractions that were active against MSSA also inhibited biofilm formation of MRSA. *Stylostichon plumosum* was the only sponge species to show activity against MRSA, MSSA, and *L. monocytogenes*, though the activity was associated with different fractions.

### *Mycale contarenii* sponge fractions affect cell–cell interaction stages of biofilm formation

$F_{md}$  of sponge *M. contarenii* was selected for further analysis due to its strong anti-biofilm activity against both MRSA and MSSA (Fig. 1a and b). Microscopy was used to investigate whether *M. contarenii* ( $F_{md}$ ) reduces MRSA biofilm formation by interfering with the initial attachment of the bacteria to the substratum (Fig. 2). After 1 h, similar numbers of treated, untreated, and  $\Delta fnbAB$  bacterial cells were attached to the polystyrene substratum (Fig. 2a, d, and g). After 4 and 7 h, confluent and multi-layered untreated cells consistent with bacterial cell–cell interactions and biofilm formation were observed (Fig. 2e and f), in contrast to the dispersed monolayer distribution of treated MRSA and the  $\Delta fnbAB$  mutant (Fig. 2b, c, h, and i). As cell-to-cell attachment, and therefore biofilm formation, by the *fnbAB* double mutant is impaired (O'Neill et al. 2008), this suggests that *M. contarenii* ( $F_{md}$ ) also affects cell–cell interactions, rather than initial attachment of bacteria to the substratum.

### Sub-fractionation of $F_{md}$ of *M. contarenii* and structural analysis of components

Sub-fractionation of *M. contarenii* ( $F_{md}$ ) was performed to identify the active components responsible for biofilm inhibition. Since the fraction contains mostly non-polar compounds, the chromatographic separation was performed by phenyl hexyl column-based HPLC (Long et al. 2008). This separation led to the isolation of eight sub-fractions (Fig. S1), three of which (P3, P7, and P8) were active at a concentration of 125  $\mu\text{g ml}^{-1}$  causing 41, 63, and 69% reduction of MRSA biofilm, respectively. At a concentration of 60  $\mu\text{g ml}^{-1}$  P7

and P8 caused 20 and 58% biofilm reduction, respectively. NMR analysis of these sub-fractions revealed the presence of unsaturated fatty acids. Due to the complex structure of these fatty acids, further structural analysis was performed using gas chromatograph/mass spectroscopy (GC-MS) to identify the active anti-biofilm component(s) (Fig. S2 and Table S4). Twenty-four metabolites with intensity >5000 units were found in *M. contarenii* ( $F_{md}$ ), ten of which were classified as major metabolites (intensity >40 000 units) (Table 2). Six of these metabolites were also present in each of the three bioactive sub-fractions at >5000 intensity units, including myristic acid, palmitic acid, and oleic acid (Table 2). These three fatty acids, along with the structurally related stearic acid, which was present in two sub-fractions, were selected for biological investigation.

### Myristic acid and oleic acid inhibit biofilm formation of MRSA and MSSA

Commercial preparations of the four fatty acids (myristic C14:0, palmitic C16:0, stearic C18:0, and oleic acid C18:1  $n = 9$ ) were investigated for their anti-biofilm properties. Myristic, palmitic, and stearic acid are unsaturated fatty acids differing in the length of their carbon chain, while oleic acid has a single double bond at C9. The two larger unsaturated fatty acids, palmitic and stearic acid, did not show any significant anti-biofilm activity even at 100  $\mu\text{g ml}^{-1}$ . Myristic and oleic acid did possess anti-biofilm activity against both MRSA and MSSA (Fig. 3). Myristic acid exhibited stronger activity against MRSA by inhibiting 79, 73, and 38% biofilm compared to 70, 57, and 28% MSSA biofilm inhibition at 100, 50, and 25  $\mu\text{g ml}^{-1}$ , respectively. Oleic acid showed stronger anti-biofilm activity against MSSA with 90, 88 and 66% inhibition compared to 96, 77, and 0% inhibition against MRSA at 100, 50, and 25  $\mu\text{g ml}^{-1}$ , respectively. We therefore proceeded with further assessing the characteristics of myristic and oleic acid.

To substantiate the specific anti-virulence properties of myristic and oleic acid, we determined whether the fatty acids affect growth of *S. aureus* (Fig. 4). Neither fatty acid eliminated the growth of MRSA or MSSA at the concentrations tested, indicating an MIC > 100  $\mu\text{g ml}^{-1}$ . However, at 100  $\mu\text{g ml}^{-1}$ , myristic acid reduced the exponential growth rate of both MRSA and MSSA and reduced bacterial stationary phase biomass after 14 h to a final OD<sub>600</sub> of 0.65 and 0.61, respectively, compared to the controls (0.93 and 0.90 OD<sub>600</sub>, respectively). A similar, though lesser, effect occurred with 50  $\mu\text{g ml}^{-1}$  myristic acid. There was minimal influence on growth of either pathogen in the presence of 25  $\mu\text{g ml}^{-1}$  myristic acid. At all the concentrations tested, oleic acid extended the lag phase of MRSA by around 2 h and reduced the exponential growth rate, but with only a minimal effect on final biomass, and for this reason the effect of oleic acid on MRSA was not investigated further. This finding is in line with a previous study that demonstrated that oleic acid delayed planktonic growth of *S. aureus* (Lee et al. 2017). In contrast, minimal effects on the exponential growth rate and biomass accumulation of MSSA were observed for oleic acid. These results indicate that inhibition of MRSA biofilm by myristic acid and inhibition of MSSA biofilm by either fatty acid at 25  $\mu\text{g ml}^{-1}$  is specifically an anti-virulence property and not directly attributable to growth inhibition or growth rate reduction.

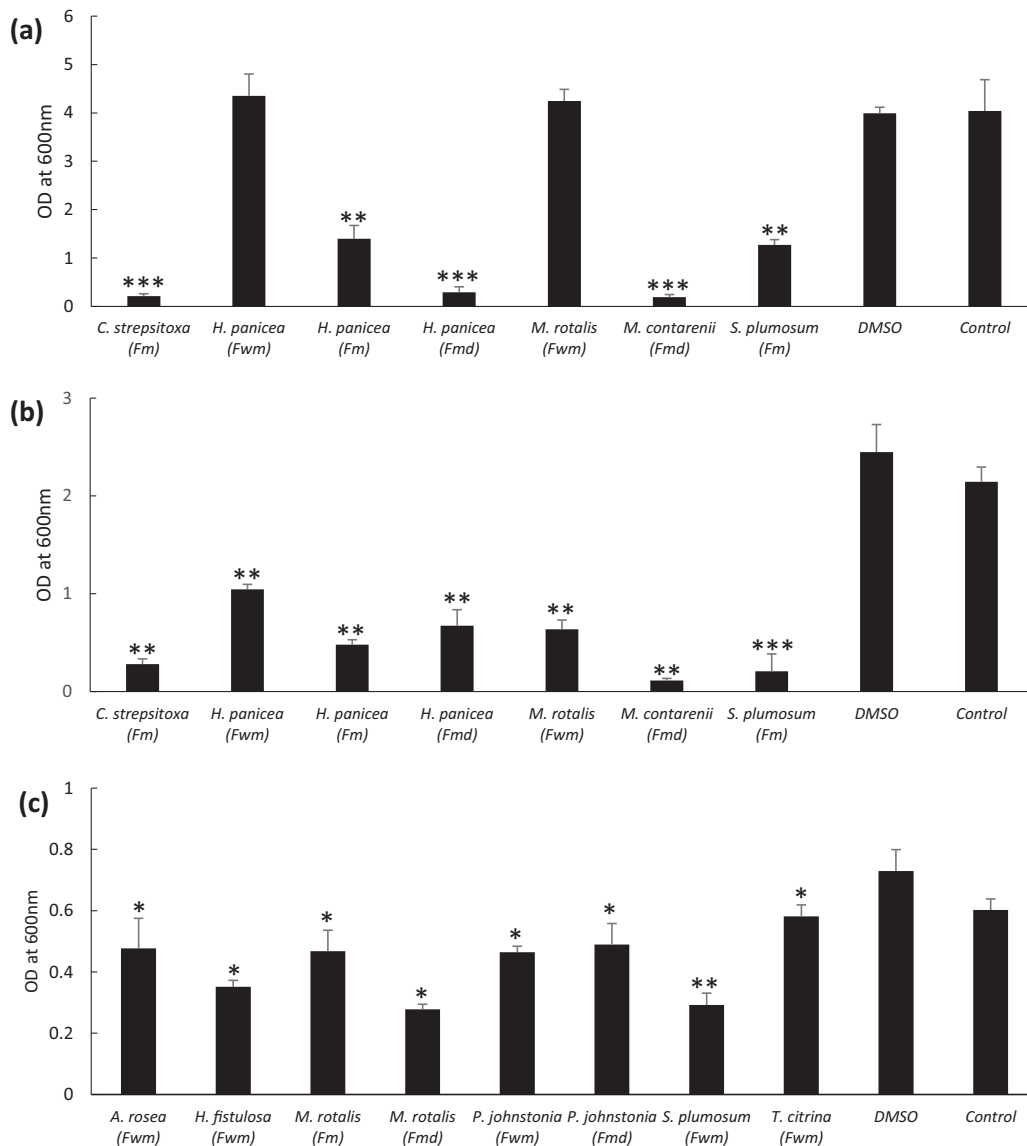


**Figure 1.** Biofilm inhibition of MRSA (a), MSSA (b), and *L. monocytogenes* (c) by sponge fractions. Bacteria were cultured with 100  $\mu\text{g ml}^{-1}$  sponge fractions or with equivalent volume of DMSO (1%). Biofilm formed after 24 h incubation at 37°C was stained with crystal violet and after solubilization, the OD<sub>600</sub> was measured. Results presented are the average  $\pm$  SD of three independent experiments performed in triplicate. \* $P < .05$ , \*\* $P < .01$ , \*\*\* $P < .001$ .

### Time-course inhibition of biofilm formation of MRSA and MSSA by myristic and oleic acid

The effect of fatty acids on biofilm formation was investigated in a dose- and time-dependent manner. Fatty acids were applied at concentrations between 6.25 and 25  $\mu\text{g ml}^{-1}$ , i.e. at concentrations that do not affect bacterial growth. Biofilm was initially detected for MRSA cultures at 2 h with an OD<sub>600</sub> of 0.46 (Fig. 5a). Steady increases in biofilm were detected after 4 h and reached OD<sub>600</sub> of 4.64 by 7 h. After 2 and 3 h, myristic acid reduced MRSA biofilm by 38%–50%, and after 4 and 5 h there was 77%–91% reduction with greater inhibition at higher concentrations. Likewise, myristic acid inhibited 78%, 74%, and 60% biofilm by 6 h and 84%, 79%, and 71% by 7 h at 25, 12.5, and 6.25  $\mu\text{g ml}^{-1}$ , respectively.

MSSA biofilm started to form at 2 h (0.74 OD<sub>600</sub>) and increased rapidly to reach 5.06 OD<sub>600</sub> at 4 h, after which time

biofilm formation stabilized (Fig. 5b and c). Both myristic and oleic acids displayed similar dose-dependent and time-dependent inhibition of MSSA biofilms. At 2 h, the fatty acids inhibited biofilm formation in a dose-dependent manner with 42%, 23%, and 16% inhibition at 25, 12.5, and 6.25  $\mu\text{g ml}^{-1}$ , respectively. Between 5 and 7 h, the anti-biofilm effect of the two fatty acids was very similar with 59%–63% reduction at 25  $\mu\text{g ml}^{-1}$ , 47%–50% at 12.5  $\mu\text{g ml}^{-1}$ , and 34%–38% at 6.25  $\mu\text{g ml}^{-1}$ .

These data show that myristic and oleic acid reduce *S. aureus* biofilm by inhibition at early stages of its development. Each fatty acid was equally effective at inhibiting MSSA biofilm accumulation, while myristic acid had stronger anti-biofilm activity against MRSA than MSSA.

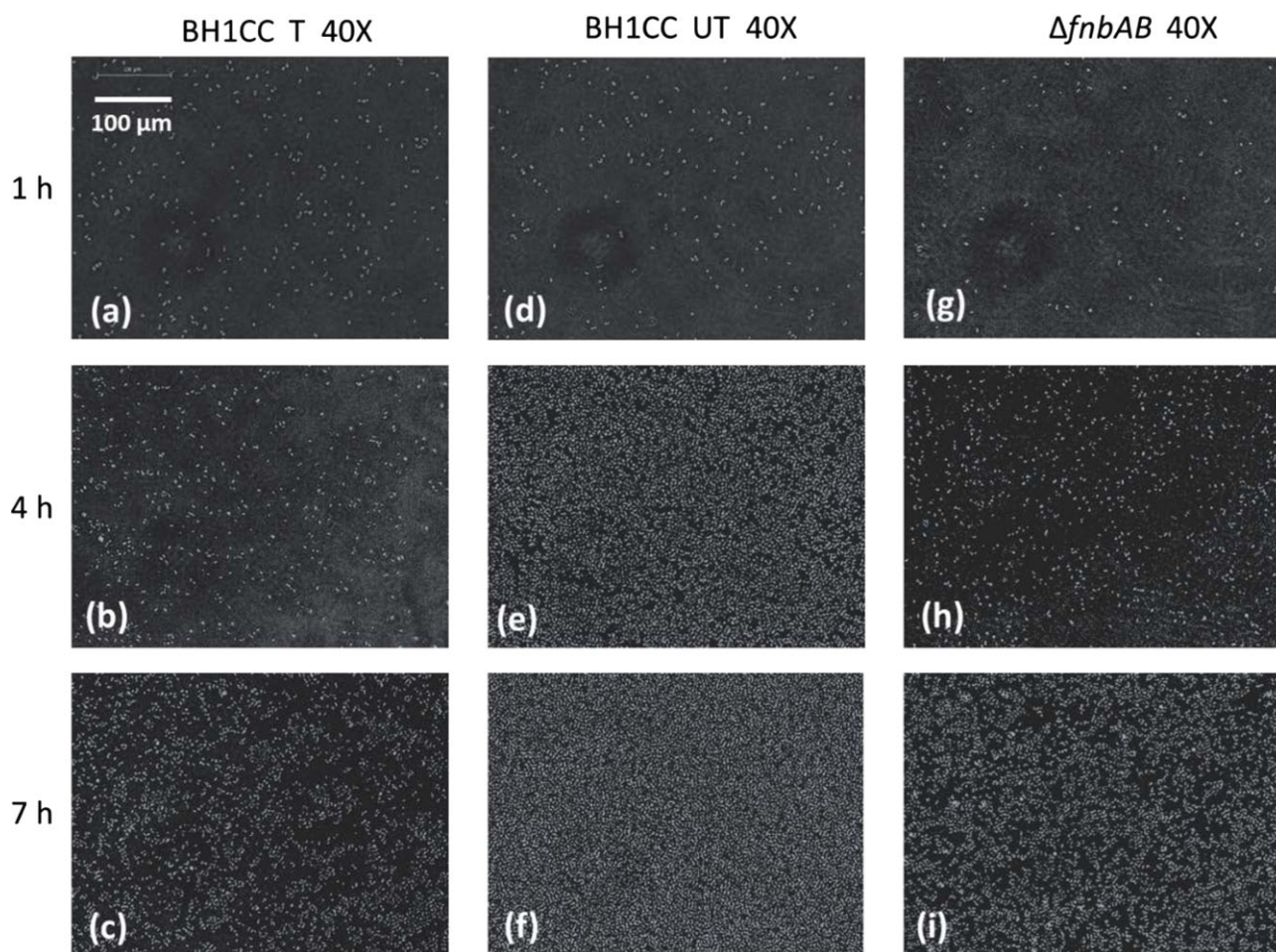


**Figure 2.** Initial stages of biofilm formation by MRSA (untreated), MRSA treated with ( $F_{md}$ ) *M. contarenii*, and MRSA  $\Delta fnbAB$ . MRSA was cultured with and without *M. contarenii* ( $F_{md}$ ) ( $100 \mu\text{g ml}^{-1}$ ), and after every hour the wells were washed and dried, and the formed biofilm was observed by microscopy. T—Treated, UT—Untreated. Scale bar— $100 \mu\text{m}$ .

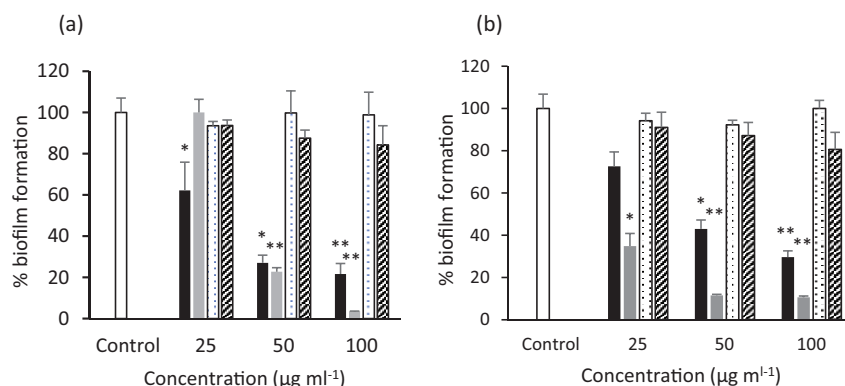


**Figure 3.** Inhibition of MRSA (a) and MSSA (b) biofilm formation by fatty acids. The assay was performed as described in Fig. 1 with the indicated concentrations of fatty acids. The 100%  $\text{OD}_{600}$  value of MRSA and MSSA controls was  $1.89 \pm 0.13$  and  $1.67 \pm 0.18$ , respectively. ■ Myristic acid, ■ Oleic acid, □ Palmitic acid, ▨ Stearic acid. \* $P < .05$ , \*\* $P < .01$ .

### Differential gene transcription induced in MRSA and MSSA by myristic acid and oleic acid

To determine the mechanism by which myristic and oleic acid inhibit biofilm formation, we investigated their effect on transcription of biofilm-related genes in MRSA and MSSA. To rule out the possibility of differential bacterial growth contributing to differential transcription,  $25 \mu\text{g ml}^{-1}$  fatty acids was

used for this experiment, and bacteria were harvested at 3 and 4 h time points as no effect on growth was observed in these conditions (Fig. 4). Moreover, the 3 and 4 h time points are just prior to, and just at, the stages when major differences in biofilm accumulation upon fatty acid treatment occurred (Fig. 5). To eliminate potential bias due to the treated bacteria forming less biofilm, total RNA was isolated from planktonic

**Table 2.** GC-MS analysis revealed components of MeOH: CH<sub>2</sub>Cl<sub>2</sub> fraction (*F<sub>md</sub>*) of sponge *M. contarenii* and its active sub-fractions (P3, P7, and P8).

Components <sup>a</sup>	<i>F<sub>md</sub></i> <sup>b</sup>	P3	P7	P8
Octanal	M			
Unknown (RI 1170)	m			
2-Undecenal	m			
Hexadecane	M		+ <sup>c</sup>	+
Pentadecanal	m			
<b>Tetradecanoic acid (myristic acid) (C<sub>14</sub>H<sub>28</sub>O<sub>2</sub>)</b>	<b>m</b>	+	+	+
Hexadecanal	M		+	
6,10,14-Trimethyl-2-pentadecanone	m		+	
Hexadecan-1-ol	M	+	+	+
Heptadecanal	M	+	+	
<b>Hexadecanoic acid (palmitic acid) (C<sub>16</sub>H<sub>32</sub>O<sub>2</sub>)</b>	<b>M</b>	+	+	+
9-Octadecenal	m		+	+
Long alkyl chain carboxylic acid isomer	m	+	+	
9-Octadecenal isomer	M			+
<b>9-Octadecenoic acid (oleic acid) (C<sub>18</sub>H<sub>34</sub>O<sub>2</sub>)</b>	<b>m</b>	+	+	+
<b>Octadecanoic acid (stearic acid) (C<sub>18</sub>H<sub>36</sub>O<sub>2</sub>)</b>	<b>m</b>	+		+
Unknown (RI 2213)	M			+
2,3-Dihydroxypropyl-9-octadecenoate (oleic acid monoglyceride)	M	+	+	+
Unknown (RI 2298)	m			+
Unknown (RI 2303)	m		+	+
2,4-Docosadienal	M			+
Bis(2-ethylhexyl)-13-benzenedicarboxylate (phthalate derivative)	m	+	+	+
Diterpene	M			+
Unknown (RI 2478)	m		+	+

<sup>a</sup>RI = Retention index (see Table S4); compounds selected for further investigation are in bold.

<sup>b</sup>m = presence of compound in *F<sub>md</sub>* with intensity >5000 units; M = major metabolite in *F<sub>md</sub>* with intensity >40 000 units.

<sup>c</sup>+ = presence of compound in sub-fraction (P3, P7, and/or P8) with intensity >5000 units; Empty cell = compound with intensity <5000 units in sub-fraction.

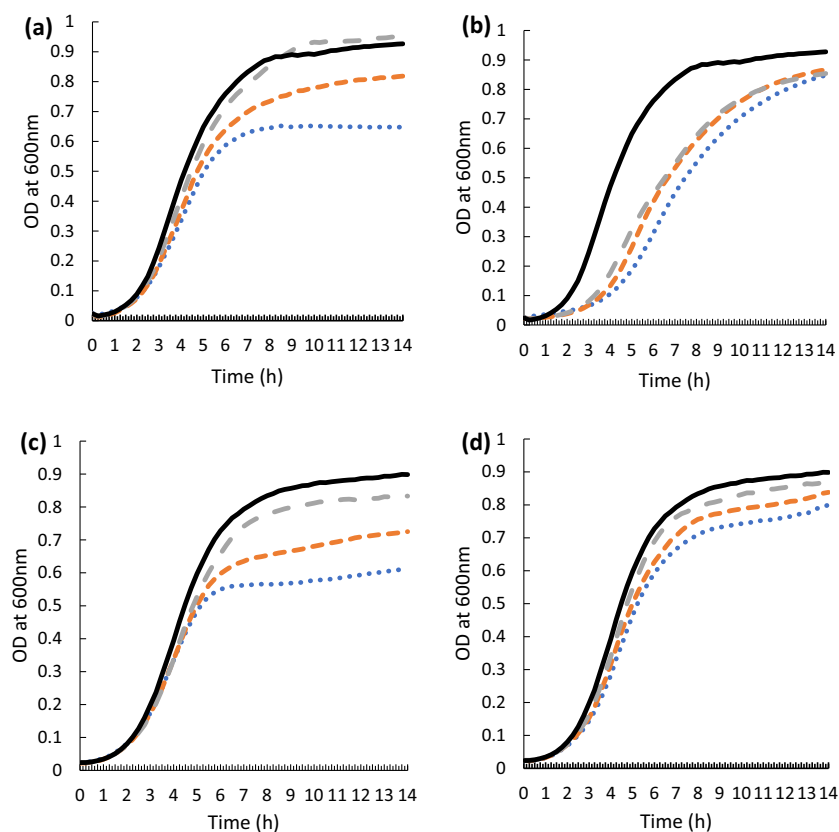


**Figure 4.** Effect of myristic acid and oleic acid on growth of MRSA and MSSA. MRSA with myristic acid (a), MRSA with oleic acid (b), MSSA with myristic acid (c), and MSSA with oleic acid (d). MRSA and MSSA (inoculum: 0.02 OD<sub>600</sub>) were grown in a 96-well plate at 37°C in the presence and absence of fatty acids at concentrations of 25–100 µg ml<sup>-1</sup> for 14 h. — Control, — 25 µg ml<sup>-1</sup>, — 50 µg ml<sup>-1</sup>, — 100 µg ml<sup>-1</sup>. Cell growth was measured by using optical density at 600 nm at 15-min intervals. Experiment was performed thrice in triplicate.

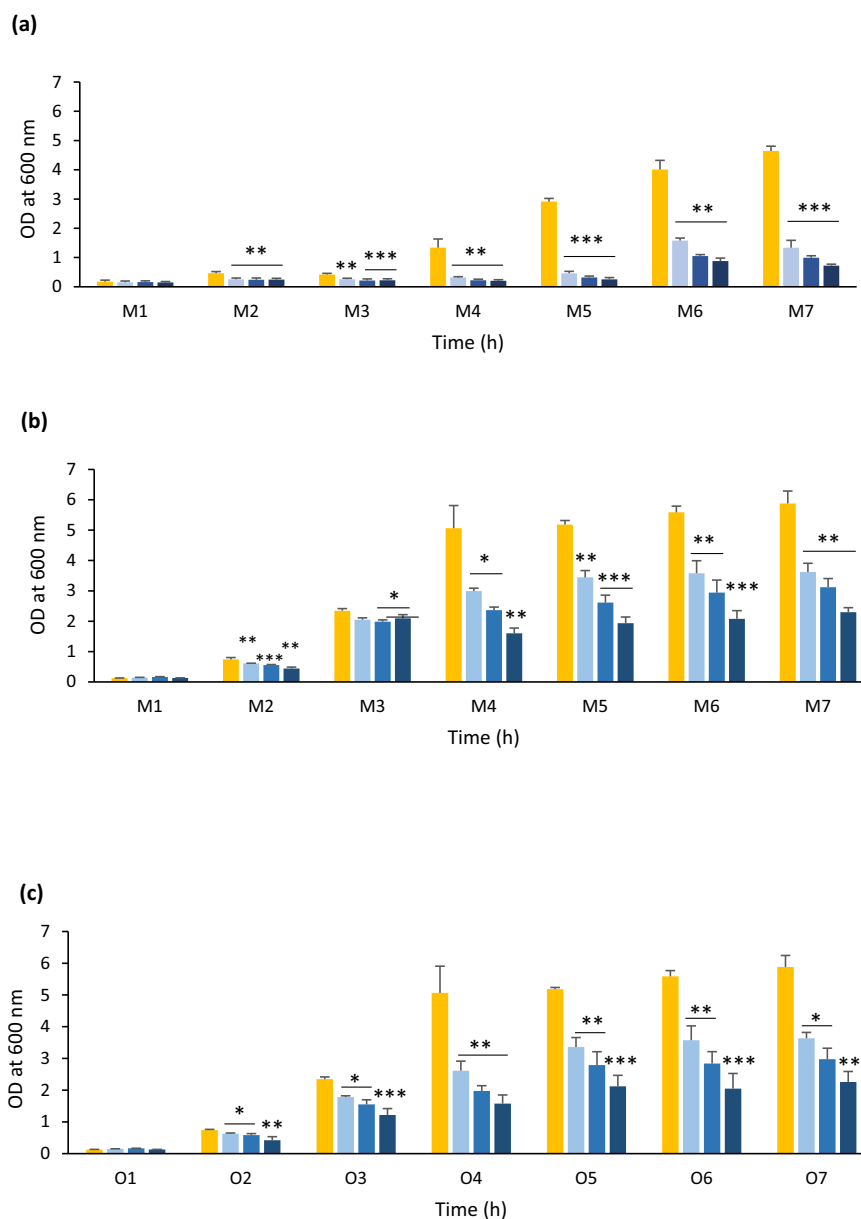


**Figure 5.** Time-course of anti-biofilm activity of myristic acid and oleic acid against MRSA and MSSA. MRSA with myristic acid (a), MSSA with myristic acid (b), and MSSA with oleic acid (c). The assay was performed as described in Fig. 1 with the indicated concentrations of oleic and myristic acid and with biofilm quantified each hour up to 7 h of culture. Results presented are the average  $\pm$  SD of three independent experiments performed in triplicate. ■ 25  $\mu\text{g ml}^{-1}$ , ■ 12.5  $\mu\text{g ml}^{-1}$ , ■ 6.25  $\mu\text{g ml}^{-1}$ , ■ Control. \* $P < .05$ , \*\* $P < .01$ , \*\*\* $P < .001$ .

bacteria grown statically in biofilm culture conditions. Quantitative real-time PCR was used to compare transcript levels of the biofilm-related genes *fnbA*, *fnbB*, *icaA*, *icaR*, *sarA*, and *agrB*. Fold change  $\geq 1.5$  was considered a differential change in transcription.

Analysis of the qPCR data revealed that myristic acid down-regulated transcription of both *fnbA* and *fnbB* in MRSA by 5.3-fold compared to the untreated culture at 3 h (Fig. 6a), whereas, by 4 h, only the expression of *fnbB* was significantly down-regulated with 1.5-fold decrease compared to control. While investigating the effect of myristic acid on biofilm-related gene transcription in MSSA, we observed no

significant change in transcript levels of *icaA* and *icaR* after 3 h (Fig. 6b); however, at 4 h, there was a 2-fold decrease in *icaA* transcription. In addition, oleic acid repressed the mRNA level of *icaA* in MSSA at 3 and 4 h with 3.2-fold change (Fig. 6c). No significant difference was observed in the transcript level of the other biofilm-related gene *icaR* in MSSA. Finally, transcription levels of *sarA* or *agrB* in MSSA or MRSA were also unchanged in the presence of either fatty acid.

In conclusion, myristic acid down-regulated transcription of the *fnbA* and *fnbB* genes in MRSA, and myristic acid and oleic acid down-regulated transcription of the *icaA* gene in MSSA.

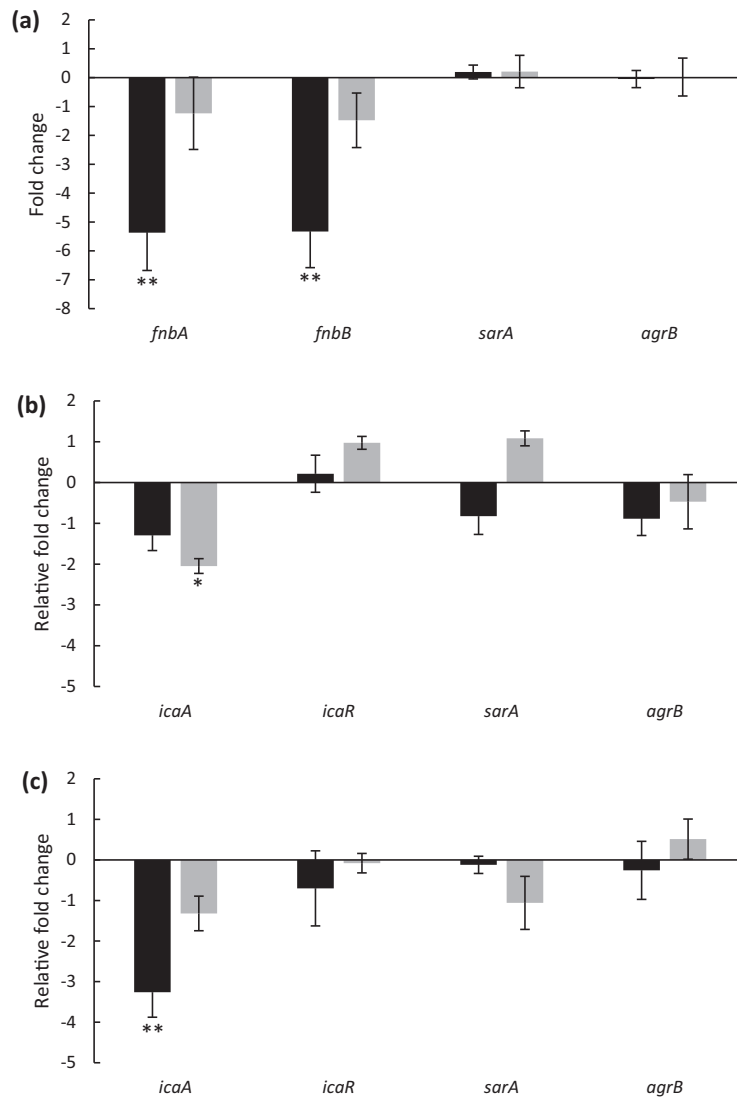


**Figure 6.** Transcriptional profiles of biofilm-related genes in *S. aureus* treated with fatty acids. Myristic acid-treated MRSA (a), myristic acid-treated MSSA (b), and oleic acid-treated MSSA (c). Comparison of relative *fnbA*, *fnbB*, (MRSA), *icaA*, *icaR* (MSSA), *sarA*, and *agrB* (MRSA and MSSA) gene transcription by RT-PCR in bacterial culture grown for 3 or 4 h in BHI medium or BHI medium supplemented with  $25 \mu\text{g ml}^{-1}$  fatty acids. The experiment was conducted with three biological and two technical replicates for each sample. ■ 3 and ■ 4 h. Fold change is relative to untreated culture. \* $P < .05$ , \*\* $P < .01$ .

## Discussion

In this study, we demonstrated that anti-biofilm activity is a prevalent characteristic of marine sponges and that sponge AVM can be exploited to inhibit biofilm formation of clinical pathogens. Out of 56 fractions prepared from 26 sponge species collected off the Irish coasts, 15 fractions from eight sponge species (27% of fractions and 31% of species) reduced biofilm production of *S. aureus* or *L. monocytogenes*. Significantly, anti-biofilm activity was not associated with inhibition of bacterial growth. Most sponge fractions that showed activity against MSSA also inhibited biofilm formation of MRSA. The exceptions were  $F_{wm}$  of *M. rotalis* and *H. panicea*, suggesting these two fractions may possess distinct AVM that act through an alternative mechanism to inhibit biofilm formation. A similar interpretation could be proposed for the lack of overlap between fractions reducing biofilm formation of *L. monocytogenes* and

those inhibiting *S. aureus* biofilm production, further showing the diversity of bioactive AVM in sponges. There are three known classes of marine sponge metabolites, namely terpenoids, pyrrole-imidazoles, and phorbaketals, that are considered non-bactericidal biofilm inhibitors (Stowe et al. 2011, Kim et al. 2021a). Together with our data, this indicates that marine sponges possess diverse AVM specific to different pathogens.

We further explored the anti-biofilm activity of *M. con-tarenii* ( $F_{md}$ ), as it showed the strongest activity against both MRSA and MSSA. NMR and GC-MS analyses of this active fraction and its active sub-fractions revealed the major presence of several fatty acids. Two of these fatty acids, myristic and oleic acid, demonstrated strong anti-biofilm activity against MRSA and MSSA. Time-course microscopy and crystal violet staining data suggest that their AVM activity influences the phase of biofilm accumulation that occurs after

initial attachment of bacteria to the substratum. Our study demonstrated inhibition in a dose-dependent manner at concentrations that did not influence bacterial growth rates. A restricted variety of fatty acid structures sourced from natural materials inhibit biofilm of pathogenic bacteria (Wenderska et al. 2011, Ramanathan et al. 2018, Cui et al. 2019). In correlation with our data, these anti-biofilm fatty acids include oleic acid, which has activity against several pathogens, including *S. aureus*, *Streptococcus mutans*, *Acinetobacter baumannii*, and *P. aeruginosa* (Pandit et al. 2015, Lee et al. 2017, Khadke et al. 2021, Selvaraj et al. 2021). Myristic acid has been previously demonstrated to exert antimicrobial activity against some bacterial species (e.g. *S. mutans*) but not others (e.g. *S. gordonii* and *S. aureus*) (Huang et al. 2011, Kim et al. 2021b, Lee et al. 2022). Surprisingly, however, these two latter recent studies from the same research group present contrasting results for the anti-biofilm activity of myristic acid at sub-lethal concentrations, with one study claiming limited activity and other strong activity. Our study clarifies that myristic acid does have anti-biofilm activity against both MRSA and MSSA. Myristic acid also has other anti-virulence activities. It inhibits hyphal and biofilm formation by the fungus *Candida albicans* (Prasath et al. 2019) and inhibits swarming motility of *Proteus mirabilis* (Liaw et al. 2004). Further investigation of myristic acid is warranted to exploit its full potential as an AVM against pathogenic microorganisms.

Investigating the mechanism of action of fatty acids on a transcriptional level revealed that myristic acid induced changes in transcription of biofilm-related genes in both MRSA and MSSA. In MRSA, myristic acid down-regulated transcription of the *fnbA* and *fnbB* genes, which encode proteins involved in bacterial cell-to-cell attachment during biofilm accumulation (McCourt et al. 2014), suggesting that this is the mechanism by which myristic acid leads to the biofilm inhibition of MRSA.

Both myristic and oleic acid down-regulated *icaA* transcription in MSSA. The *ica* operon encodes proteins for the biosynthesis of the PIA polysaccharide that facilitates cell aggregation, thereby enhancing biofilm formation in MSSA (McCarthy et al. 2015). In support of this finding, anti-biofilm activity of rhodomyltone extracted from *Rhodomyrtus tomentosa* leaves inhibited transcription of *S. aureus ica* gene (Saising et al. 2015). We propose that the anti-biofilm ability of myristic acid is due to its down-regulation of transcription of distinct biofilm genes in both MRSA and MSSA. Further study would examine the ability of fatty acids to not only prevent biofilm formation but also to eradicate pre-formed biofilms.

In conclusion, we report strong anti-biofilm activity of marine sponge fractions against clinical pathogens MRSA, MSSA, and *L. monocytogenes*. Myristic and oleic acid were identified as the active AVM of *M. contarenii* ( $F_{md}$ ) that inhibited *S. aureus* biofilm formation. The other active sponge fractions constitute an important resource for the future exploration of additional AVM. Transcriptome analysis revealed molecular targets of myristic and oleic acid: suppression of transcription of genes related to intercellular attachment and biofilm accumulation in both MRSA and MSSA. This study indicates that fatty acids are promising candidates for development of AVM. They could be used as coating on medical implantable de-

vices and in food processing facilities to prevent biofilm accumulation.

## Acknowledgements

The authors thank Daniel Rodrigues (University of Galway) for his contribution to the collection of the sponge specimens. Sponge species were identified by Daniel Rodrigues and the sponge taxonomist Dr Christine Morrow (University of Galway). We thank Dr Laurence Jennings (University of Galway) for supervision of the purification work and Dr Laura Gallagher (University of Galway) for her advice and support with biofilm experiments.

## Supplementary data

Supplementary data is available at *JAMBIO Journal* online.

## Conflict of interest

None declared.

## Funding

This project was funded through the Irish Research Council under a Government of Ireland Postgraduate Scholarship held by Neyaz Khan (GOIPG/2017/910). Part of this project (Grant-Aid Agreement Nos. PBA/MB/16/01) was carried out with the support of the Marine Institute and is funded under the Marine Research Program by the Irish Government. Additional support was provided by the Irish Higher Education Authority as part of a COVID-19 costed extension programme.

## Author contributions

Neyaz A. Khan (Conceptualization, Data curation, Formal analysis, Funding acquisition, Investigation, Methodology, Validation, Visualization, Writing – original draft, Writing – review & editing), Nicolas Barthes (Data curation, Formal analysis, Investigation, Methodology, Validation, Visualization, Writing – review & editing), Grace McCormack (Conceptualization, Funding acquisition, Supervision, Writing – review & editing), James P. O’Gara (Methodology, Resources, Writing – review & editing), Olivier P. Thomas (Conceptualization, Funding acquisition, Resources, Supervision, Writing – review & editing), and Aoife Boyd (Conceptualization, Data curation, Funding acquisition, Methodology, Project administration, Resources, Supervision, Validation, Writing – original draft, Writing – review & editing)

## Data availability

The data underlying this article are available in the article and in its online [supplementary material](#).

## References

- Blair JM. A climate for antibiotic resistance. *Nature Clim Change* 2018;8:460–1. <https://doi.org/10.1038/s41558-018-0183-0>.
- Boles BR, Horswill AR. Agr-mediated dispersal of *Staphylococcus aureus* biofilms. *PLoS Pathog* 2008;4:e1000052. <https://doi.org/10.1371/journal.ppat.1000052>.

- Cafiso V, Bertuccio T, Santagati M et al. Presence of the *ica* operon in clinical isolates of *Staphylococcus epidermidis* and its role in biofilm production. *Clin Microbiol Infect* 2004;10:1081–8. <https://doi.org/10.1111/j.1469-0691.2004.01024.x>.
- Chen M, Yu Q, Sun H. Novel strategies for the prevention and treatment of biofilm related infections. *Int J Mol Sci* 2013;14:18488–501. <https://doi.org/10.3390/ijms140918488>.
- Chien Y-T, Manna A, Projan S et al. SarA, a global regulator of virulence determinants in *Staphylococcus aureus*, binds to a conserved motif essential for sar-dependent gene regulation. *J Biol Chem* 1999;274:37169–76. <https://doi.org/10.1074/jbc.274.52.37169>.
- CLSI. *Performance Standards for Antimicrobial Disk Susceptibility Tests; Approved standard—CLSI document M02-A12*. 12th edn. Wayne, PA: Clinical and Laboratory Standards Institute. 2015.
- Cue D, Lei MG, Luong TT et al. Rbf promotes biofilm formation by *Staphylococcus aureus* via repression of IcaR, a negative regulator of *ica*ABCD. *J Bacteriol* 2009;191:6363–73. <https://doi.org/10.1128/JB.00913-09>.
- Cui C, Song S, Yang C et al. Disruption of quorum sensing and virulence in *Burkholderia cenocepacia* by a structural analogue of the cis-2-dodecenoic acid signal. *Appl Environ Microbiol* 2019;85:e00105–19. <https://doi.org/10.1128/AEM.00105-19>.
- Fitzpatrick F, Humphreys H, O’Gara J. Environmental regulation of biofilm development in methicillin-resistant and methicillin-susceptible *Staphylococcus aureus* clinical isolates. *J Hosp Infect* 2006;62:120–2. <https://doi.org/10.1016/j.jhin.2005.06.004>.
- Galie S, García-Gutiérrez C, Miguélez EM et al. Biofilms in the food industry: health aspects and control methods. *Front Microbiol* 2018;9:898. <https://doi.org/10.3389/fmicb.2018.00898>.
- Glaser P, Frangeul L, Buchrieser C et al. Comparative genomics of *Listeria species*. *Science* 2001;294:849–52. <https://doi.org/10.1126/science.1063447>.
- Holloway BW. Genetic recombination in *Pseudomonas aeruginosa*. *J Gen Microbiol* 1955;13:572–81. <https://doi.org/10.1099/00221287-13-3-572>.
- Huang C, Alimova Y, Myers T et al. Short- and medium-chain fatty acids exhibit antimicrobial activity for oral microorganisms. *Arch Oral Biol* 2011;56:650–4. <https://doi.org/10.1016/j.archoralbio.2011.01.011>.
- Huigens RW, Richards JJ, Parise G et al. Inhibition of *Pseudomonas aeruginosa* biofilm formation with bromoageliferin analogues. *J Am Chem Soc* 2007;129:6966–7. <https://doi.org/10.1021/ja069017t>.
- Jennings L, Khan N, Kaur N et al. Brominated bisindole alkaloids from the Celtic Sea sponge *Spongosorites calcicola*. *Molecules* 2019, 24:3890. <https://doi.org/10.3390/molecules24213890>.
- Khadke SK, Lee J-H, Kim Y-G et al. Assessment of antibiofilm potencies of nervonic and oleic acid against *Acinetobacter baumannii* using in vitro and computational approaches. *Biomedicines* 2021;9:1133. <https://doi.org/10.3390/biomedicines9091133>.
- Khan NA, Kaur N, Owens P et al. Bis-indole alkaloids isolated from the sponge *Spongosorites calcicola* disrupt cell membranes of MRSA. *Int J Mol Sci* 2022;23:1991. <https://doi.org/10.3390/ijms23041991>.
- Kim Y-G, Lee J-H, Lee S et al. Antibiofilm activity of phorbaketals from the marine sponge *Phorbasp. sp.* against *Staphylococcus aureus*. *Marine Drugs* 2021a;19:301. <https://doi.org/10.3390/md19060301>.
- Kim YG, Lee JH, Park S et al. Inhibition of polymicrobial biofilm formation by saw palmetto oil, lauric acid and myristic acid. *Microb Biotechnol* 2021b;15:590–602. <https://doi.org/10.1111/1751-7915.13864>.
- Laport M, Santos O, Muricy G. Marine sponges: potential sources of new antimicrobial drugs. *Curr Pharm Biotechnol* 2009;10:86–105. <https://doi.org/10.2174/138920109787048625>.
- Lee JH, Kim YG, Lee J. Inhibition of *Staphylococcus aureus* biofilm formation and virulence factor production by petroselinic acid and other unsaturated C18 fatty acids. *Microbiol Spectr* 2022;10:e0133022. <https://doi.org/10.1128/spectrum.01330-22>.
- Lee J-H, Kim Y-G, Park JG et al. Supercritical fluid extracts of *Moringa oleifera* and their unsaturated fatty acid components inhibit biofilm formation by *Staphylococcus aureus*. *Food Control* 2017;80:74–82. <https://doi.org/10.1016/j.foodcont.2017.04.035>.
- Liaw S-J, Lai H-C, Wang W-B. Modulation of swarming and virulence by fatty acids through the RsbA protein in *Proteus mirabilis*. *Infect Immun* 2004;72:6836–45. <https://doi.org/10.1128/IAI.72.12.6836-6845.2004>.
- Long W, Henderson JW, Joseph M. Comparing selectivity of phenylhexyl and other types of phenyl bonded phases. *LC GC North America* 2008, 49–49. <http://www.chromatographyonline.com/comparing-selectivity-phenylhexyl-and-other-types-phenyl-bonded-phases> (14 February 2022, date last accessed).
- Makino K, Oshima K, Kurokawa K et al. Genome sequence of *Vibrio parahaemolyticus*: a pathogenic mechanism distinct from that of *V. cholerae*. *Lancet* 2003;361:743–9. [https://doi.org/10.1016/S0140-6736\(03\)12659-1](https://doi.org/10.1016/S0140-6736(03)12659-1).
- Masters JR. Hela cells 50 years on: the good, the bad and the ugly. *Nat Rev Cancer* 2002;2:315–9. <https://doi.org/10.1038/nrc775>.
- Matlawska-Wasowska K, Finn R, Mustel A et al. The *Vibrio parahaemolyticus* type III secretion systems manipulate host cell MAPK for critical steps in pathogenesis. *BMC Microbiol* 2010;10:1–16. <https://doi.org/10.1186/1471-2180-10-329>.
- Mccarthy H, Rudkin JK, Black NS et al. Methicillin resistance and the biofilm phenotype in *Staphylococcus aureus*. *Front Cell Infect Microbiol* 2015;5:1. <https://doi.org/10.3389/fcimb.2015.00001>.
- McCourt J, O’Halloran D, McCarthy H et al. Fibronectin-binding proteins are required for biofilm formation by community-associated methicillin-resistant *Staphylococcus aureus* strain LAC. *FEMS Microbiol Lett* 2014;353:157–64. <https://doi.org/10.1111/1574-6968.12424>.
- Novick R. Properties of a cryptic high-frequency transducing phage in *Staphylococcus aureus*. *Virology* 1967;33:155–66. [https://doi.org/10.1016/0042-6822\(67\)90105-5](https://doi.org/10.1016/0042-6822(67)90105-5).
- O’Neill E, Pozzi C, Houston P et al. Association between methicillin susceptibility and biofilm regulation in *Staphylococcus aureus* isolates from device-related infections. *J Clin Microbiol* 2007;45:1379–88. <https://doi.org/10.1128/JCM.02280-06>.
- O’Neill E, Pozzi C, Houston P et al. A novel *Staphylococcus aureus* biofilm phenotype mediated by the fibronectin-binding proteins, FnBPA and FnBPB. *J Bacteriol* 2008;190:3835–50. <https://doi.org/10.1128/JB.00167-08>.
- Pandit S, Cai J, Song K et al. Identification of anti-biofilm components in *Withania somnifera* and their effect on virulence of *Streptococcus mutans* biofilms. *J Appl Microbiol* 2015;119:571–81. <https://doi.org/10.1111/jam.12851>.
- Percival SL, Suleman L, Vuotto C et al. Healthcare-associated infections, medical devices and biofilms: risk, tolerance and control. *J Med Microbiol* 2015;64:323–34. <https://doi.org/10.1099/jmm.0.000032>.
- Pfaffl MW. A new mathematical model for relative quantification in real-time RT-PCR. *Nucl Acids Res* 2001;29:e45. <https://doi.org/10.1093/nar/29.9.e45>.
- Picton BE, Morrow CC. Encyclopedia of marine life of Britain and Ireland. [www.habitas.org.uk/marinelife/](http://www.habitas.org.uk/marinelife/) (15 May 2022, date last accessed).
- Pluskal T, Castillo S, Villar-Briones A et al. Mzmine 2: modular framework for processing, visualizing, and analyzing mass spectrometry-based molecular profile data. *BMC Bioinf* 2010;11:1–11. <https://doi.org/10.1186/1471-2105-11-395>.
- Prasath K, Sethupathy S, Pandian S. Proteomic analysis uncovers the modulation of ergosterol, sphingolipid and oxidative stress pathway by myristic acid impeding biofilm and virulence in *Candida albicans*. *J Proteomics* 2019;208:103503. <https://doi.org/10.1016/j.jprot.2019.103503>.
- Ramakers C, Ruijter JM, Deprez RHL et al. Assumption-free analysis of quantitative real-time polymerase chain reaction (PCR) data. *Neurosci Lett* 2003;339:62–66. [https://doi.org/10.1016/S0304-3940\(02\)01423-4](https://doi.org/10.1016/S0304-3940(02)01423-4).
- Ramanathan S, Ravindran D, Arunachalam K et al. Inhibition of quorum sensing-dependent biofilm and virulence genes expression in

- environmental pathogen *Serratia marcescens* by petroselinic acid. *Antonie Van Leeuwenhoek* 2018;111:501–15. <https://doi.org/10.1007/s10482-017-0971-y>.
- Rogers SA, Huigens III, R. W *et al.* Synergistic effects between conventional antibiotics and 2-aminoimidazole-derived antibiofilm agents. *Antimicrob Agents Chemother* 2010;54:2112–8. <https://doi.org/10.1128/AAC.01418-09>.
- Rozen S, Skaletsky H Primer3 on the www for general users and for biologist programmers. In: Misener S, Krawetz S A (eds.), *Bioinformatics Methods and Protocols. Methods Mol Biol*. Totowa, NJ: Humana Press, 2000, 365–86. <https://doi.org/10.1385/1-59259-192-2:365>.
- Saising J, Götz F, Dube L *et al.* Inhibition of Staphylococcal biofilm-related gene transcription by rhodomyrone, a new antibacterial agent. *Ann Microbiol* 2015;65:659–65. <https://doi.org/10.1007/s13213-014-0904-1>
- Scallan E, Hoekstra R, Angulo F *et al.* Foodborne illness acquired in the United States—major pathogens. *Emerg Infect Dis* 2011;17:7. <https://doi.org/10.3201/eid1701.P11101>
- Selvaraj A, Valliammai A, Premika M *et al.* *Sapindus mukorossi* Gaertn. and its bioactive metabolite oleic acid impedes methicillin-resistant *Staphylococcus aureus* biofilm formation by down regulating adhesion genes expression. *Microbiol Res* 2021;242:126601. <https://doi.org/10.1016/j.micres.2020.126601>
- Serra R, Grande R, Butrico L *et al.* Chronic wound infections: the role of *Pseudomonas aeruginosa* and *Staphylococcus aureus*. *Expert Rev Anti Infect Ther* 2015;13:605–13. <https://doi.org/10.1586/147872.10.2015.1023291>.
- Stowe S, Richards J, Tucker A *et al.* Anti-biofilm compounds derived from marine sponges. *Marine Drugs* 2011;9:2010–35. <https://doi.org/10.3390/md9102010>
- Taschner S, Meinke A, von Gabain A *et al.* Selection of peptide entry motifs by bacterial surface display. *Biochem J* 2002;367:393–402. <https://doi.org/10.1042/bj20020164>
- Vergara-Irigaray M, Valle J, Merino N *et al.* Relevant role of fibronectin-binding proteins in *Staphylococcus aureus* biofilm-associated foreign-body infections. *Infect Immun* 2009;77:3978–91. <https://doi.org/10.1128/IAI.00616-09>
- Vuong C, Saenz HL, Götz F *et al.* Impact of the agr quorum-sensing system on adherence to polystyrene in *Staphylococcus aureus*. *J Infect Dis* 2000;182:1688–93. <https://doi.org/10.1086/317606>
- Wenderska IB, Chong M, McNulty J *et al.* Palmitoyl-dl-carnitine is a multitarget inhibitor of *Pseudomonas aeruginosa* biofilm development. *ChemBioChem* 2011;12:2759–66. <https://doi.org/10.1002/cbic.201100500>
- Werner G, Strommenger B, Witte W. Acquired vancomycin resistance in clinically relevant pathogens. *Future Microbiol* 2008;3:547–62. <https://doi.org/10.2217/17460913.3.5.547>.
- Xu Z, Liang Y, Lin S *et al.* Crystal violet and XTT assays on *Staphylococcus aureus* biofilm quantification. *Curr Microbiol* 2016;73:474–82. <https://doi.org/10.1007/s00284-016-1081-1>.